Surface Characterization of Poly(styrene-*co*-*p*-hexafluorohydroxyisopropyl-α-methylstyrene)/Poly(4-vinylpyridine) Blends Spanning the Immiscibility−Miscibility−Complexation Transition by XPS, ToF-SIMS, and AFM

Shiyong Liu,[†,‡] Chi-Ming Chan,[*,†] Lu-Tao Weng,[§] Lin Li,[†,⊥] and Ming Jiang[*,‡]

Department of Chemical Engineering, Hong Kong University of Science and Technology, Clear Water Bay, Hong Kong; Institute of Macromolecular Science and Laboratory of Molecular Engineering of Polymers, Fudan University, Shanghai, China; and Materials Characterization and Preparation Facility, Hong Kong University of Science and Technology, Clear Water Bay, Hong Kong

Received March 12, 2001; Revised Manuscript Received February 25, 2002

ABSTRACT: X-ray photoelectron spectroscopy (XPS), time-of-flight secondary ion mass spectrometry (ToF-SIMS), and atomic force microscopy (AFM) were used to investigate the surface composition, structure, and morphology of various poly(styrene-*co*-*p*-hexafluorohydroxyisopropyl-α-methylstyrene)/poly(4-vinylpyridine) (PS(OH)/PVPy) blends spanning the immiscibility−miscibility−complexation transition, when the density of the hydrogen bond was adjusted by varying the hydroxyl content of the PS(OH) component. The surface chemical composition of the blends has been shown to be strongly dependent on the density of the hydrogen bonds. XPS results revealed that the intermolecular hydrogen bonding between PS(OH) and PVPy could induce a shift of 0.9−1 and 1.2−1.3 eV in the N 1s and O 1s binding energies, respectively. ToF-SIMS data showed that the absolute intensity of positive secondary ions characteristic of PVPy at m/z = 80, 93, 106, and 120 was enhanced due to the formation of hydrogen bonds. The hydroxyl groups enhanced the formation of pyridine-ring-containing ions, which need one proton in the process of ion fragmentation. The positive ions at m/z = 132, 195, and 209, which are also characteristic of PVPy, showed little enhancement because these ions contain unsaturated double bonds. ToF-SIMS and AFM results showed that the size of the dispersed phase decreased as the density of the hydrogen bond increased.

Introduction

The surface properties of polymer blends have been the subject of many interesting studies.[1−6] Controlling of the surface composition of these materials is vital to many technologically important applications such as the adhesion of different polymeric phases,[7] colloidal stability, and the design of composites and biocompatible materials.[8] The success of these applications requires a fundamental understanding of the microstructure and composition of polymer blend surfaces. In most cases, the surface of a two-phase polymer mixture should be occupied predominately by the lower surface energy component.[9,10] Even in miscible polymer blends, the segregation of the lower surface energy component at the surface has been observed.[2,6,11]

In practice, the surface composition of polymer blends has been found to depend strongly on surface energy of the components[12−18] as well as the magnitude of the interaction between the two polymer components that determines their degree of miscibility.[15−18] Other factors that affect the surface composition of the blends are the blend composition,[3,12−19] the molecular weights of the components,[3,15,16,20] and the thickness of the blend sample.[20,21]

Binary polymer blends are in general immiscible because of weak interactions between the two components. However, when functionalities of the two polymer components strongly interact through specific interactions such as hydrogen bonding, the polymer blend can become miscible.[22,23] By gradually increasing the density of one of the specific interaction groups, not only an immiscible blend can become miscible but an interpolymer complex can also form. In this case, the two polymers form a complex that precipitates when the two constituent polymer solutions are mixed in a common solvent.[24−27] It is believed that polymer chains are randomly mixed in a miscible blend while they are paired in a complex. Thus, the changes in the surface composition, microstructure, and morphology of a polymer blend that undergoes the process of the immiscibility−miscibility−complexation transition are an extremely interesting area in the study of polymer blend surfaces.

This study considers a polymer blend system in which the functional group of one polymer component can form hydrogen bond with the other polymer component in the blend, and the concentration of this functional group can be adjusted experimentally. The proton-donating polymer poly(styrene-*co*-*p*-hexafluorohydroxyisopropyl-α-methylstyrene) (PS(OH)) (Scheme 1)−of which the hydroxyl content can be varied−was chosen. We have previously reported that the water contact angle of a series of PS(OH) copolymers decreased only slightly with the *p*-hexafluorohydroxyisopropyl-α-methylstyrene (HFMS) content, indicating that the surface free energy remained relatively unchanged and there was no fluorine segregation at the surface.[28] The decrease of surface energy due to the presence of the fluorinated groups was

[†] Department of Chemical Engineering, Hong Kong University of Science and Technology.
[‡] Fudan University.
[§] Materials Characterization and Preparation Facility, Hong Kong University of Science and Technology.
[⊥] Present address: State Key Laboratory of Polymer Physics and Chemistry, Center for Molecular Science, Institute of Chemistry, Chinese Academy of Sciences, Beijing China, 100080.
* To whom correspondence should be addressed.

10.1021/ma010435m CCC: $22.00
Published on Web 06/06/2002

Scheme 1

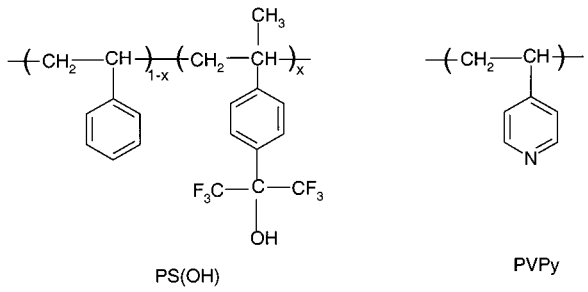

offset by the presence of the polar hydroxyl groups. Poly(4-vinylpyridine) (PVPy) (Scheme 1) is a proton-accepting polymer which is miscible with various acidic polymers through hydrogen bonding. The PS(OH)/PVPy blends undergo the immiscibility−miscibility−complexation transition as the hydroxyl content of the PS(OH) changes.

X-ray photoelectron spectroscopy (XPS) has been used to investigate the electronic structure, the surface chemical composition, and other properties of polymer blends and copolymers.[29−31] Time-of-flight secondary ion mass spectrometry (ToF-SIMS) has gained importance over the past 10 years in the characterization of polymer surfaces due to its high molecular specificity, extreme surface sensitivity, high mass resolution,[29−31] and its ability to provide detailed information on the surface molecular structure, including polymer tacticity,[32] sequence distribution,[33] end groups,[34] and the extent of branching and cross-linking.[35] In addition, the effects of the chemical interactions between the polymer components on ion formation in a SIMS process are of fundamental interest.[36,37]

In this study, XPS, ToF-SIMS, and atomic force microscopy (AFM) were used to study the surface chemical composition and structure of the PS(OH)/PVPy blend system, in particular the immiscibility−miscibility−complexation transition as the hydroxyl content of the PS(OH) changed.

Experiment

Materials. Styrene and *p*-chloro-α-methylstyrene were purified and vacuum-distilled in the presence of calcium hydride and a sodium mirror just before use. The hydroxyl-containing monomer *p*-(hexafluoro-2-hydroxyisopropyl)-α-methylstyrene (HFMS) was synthesized from *p*-chloromethylstyrene via the Grignard reaction with hexafluoroacetone.[25,28] Copolymers of styrene and HFMS were prepared by solution copolymerization in benzene at 60 °C using 2,2-azoisobutyronitrile (AIBN) as the initiator.[38] The products were purified by precipitation from a dichloromethane/petroleum ether mixture. By varying the feed composition, a series of PS(OH) polymers with the HFMS (or hydroxyl) content ranging from 1 to 49 mol % were obtained. The molecular weights of PS(OH) polymers were measured by size exclusion chromatography using tetrahydrofuran as solvent and polystyrene as the standard. The results are shown in Table 1. Their structures were verified by Fourier transform infrared spectroscopy[38] and nuclear magnetic resonance spectroscopy.[25] Each HFMS unit would be expected to be linked with the styrene units during copolymerization because α-methylstyrene is difficult to homopolymerize in free-radical polymerization due to its low ceiling temperature. The HFMS content in the copolymers was determined from the nitrogen content as measured by elemental analysis. The glass transition temperature measurements were performed with a TA 2910 differential scanning calorimeter.

PVPy was produced through radical polymerization of 4-vinylpyridine.[39] The product was purified in the methanol/ethyl ether cycle three times. The molar mass (M) of PVPy was calculated using $[\eta] = 2.5 \times 10^{-2} M^{0.68}$. The intrinsic viscosity ($[\eta]$, dL/g) was measured in absolute ethanol. Table 1 shows the physical properties of the PS(OH) copolymers and PVPy.

Table 1. Characteristic Data of Samples Used in This Study

sample code	hydroxyl content/(mol %)	$M_n/10^4$ (g/mol)	M_w/M_n	T_g (°C)
PS		1.9	1.05	98.5
PS(OH)-1	1	3.685	1.51	97.2
PS(OH)-3	3.2	4.656	1.31	99.1
PS(OH)-5	5.1	3.219	1.48	100.0
PS(OH)-8	8.3	3.870	1.52	101.3
PS(OH)-12	12.4	3.413	1.27	105.3
PS(OH)-21	20.6	2.541	1.83	112.5
PS(OH)-34	33.8	1.326	1.52	129.4
PS(OH)-49	49.2	1.047	1.61	122.2
PVPy		3.52[a]		146

[a] Determined from intrinsic viscosity.

Sample Preparation. PS(OH) copolymers and PVPy were separately dissolved in chloroform ($CHCl_3$) at a concentration of 10 g/L. A blend solution was prepared by mixing the same amount of each polymer solution with stirring. Depending on the HFMS content of the PS(OH), the mixed solutions might remain clear or form an interpolymer complex precipitate. For PS(OH)-1/PVPy, PS(OH)-3/PVPy, and PS(OH)-5/PVPy blends, clear solutions were formed and spin-cast at 3800 rpm onto silicon wafers. The film thickness was kept at about 200−230 nm using the same concentration of the solution and the same spin rate. When the HFMS content reached or exceeded 8 mol %, an interpolymer complex precipitate formed in the solutions. The precipitate was separated by centrifugation, washed with $CHCl_3$ three times, and then kept in $CHCl_3$. The chemical compositions of the precipitates were determined by fluorine elemental analysis. The slightly swollen precipitate was pressed onto a silicon wafer to form thin and smooth films. The films were then dried in a vacuum at room temperature overnight.

Surface Characterization. The surface properties of the series of PS(OH)/PVPy blends were studied using XPS, ToF-SIMS, and AFM. The XPS spectra were obtained with a PHI 5600 multitechnique system equipped with a monochromatic Al Kα X-ray source. A pass energy of 23.4 eV was used. All core-level spectra were referenced to the C 1s neutral carbon peak at 285.0 eV. The emission angle (the angle between the surface normal and the axis of the analyzer) of the photoelectrons was 45°, corresponding to a sampling depth of approximately 47 Å, assuming an attenuation length of 22 Å.[29]

ToF-SIMS measurements were performed on a Physical Electronics PHI 7200 ToF-SIMS spectrometer. The primary ions were generated from a Cs ion source (8 kV). The scanned area was 200 μm × 200 μm, and the total ion dose for each spectrum acquisition was $<4 \times 10^{11}$ ions/cm^2. Charge compensation was realized by low-energy (0−70 eV) flooding electrons being pulsed out of phase with the primary ion beam. Both positive and negative high-resolution mass spectra were recorded. The surface chemical images of the PS(OH)/PVPy blends were acquired in the negative mode using a $^{69}Ga^+$ beam at 25 kV.

Tapping mode AFM images were obtained at ambient conditions using a NanoScope III MultiMode AFM (Digital Instruments). Both height and phase images were recorded simultaneously using the retrace signal. Si tips with a resonance frequency of approximately 300 kHz and a spring constant of about 40 N m^{-1} were used, and the scan rate was in the range 0.5−1.2 Hz.

Results and Discussion

Immiscibility−Miscibility−Complexation Transition. The physical properties of the samples used in this study are summarized in Table 1. The chloroform

Table 2. Characteristic Data of PS(OH)/PVPy Blends/Complexes

sample code	feed composition (PS(OH), mol %)	bulk composition (PS(OH), mol %)	T_g (°C)	surface concentration (PS(OH), mol %)
PS/PVPy	50.2	50.2	99.0/145.5	99.6
PS(OH)-1/PVPy	49.8	49.8	104.1/143.2	89.3
PS(OH)-3/PVPy	48.9	48.9	106.5/132.4	80.8
PS(OH)-5/PVPy	48.1	48.1	117.8	70.7
PS(OH)-8/PVPy	46.9	55.2	132.2	70.4
PS(OH)-12/PVPy	45.4	52.8	149.3	60.8
PS(OH)-21/PVPy	42.7	49.9	160.4	50.9
PS(OH)-34/PVPy	38.9	46.8	166.1	44.3
PS(OH)-49/PVPy	35.3	42.6	176.5	40.5

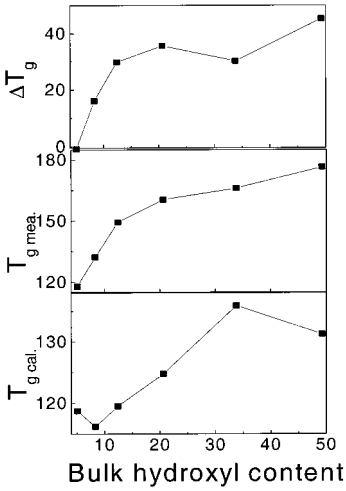

Figure 1. Calculated and measured T_g's for the PS(OH)/PVPy blends or complexes as a function of the hydroxyl content in PS(OH).

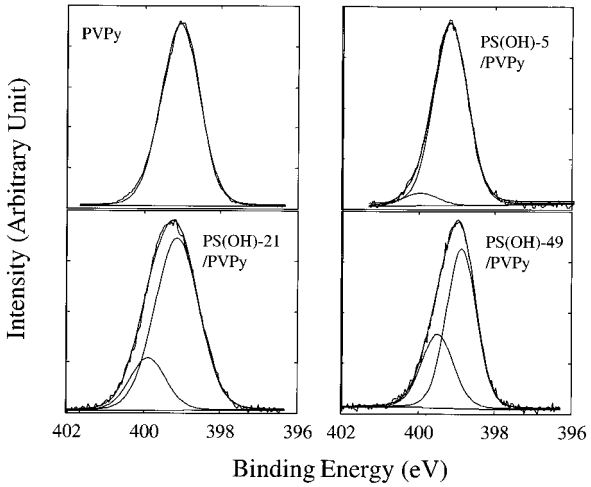

Figure 2. XPS N 1s core-level spectra of pure PVPy, the PS(OH)-5/PVPy blend, and the PS(OH)-21/PVPy and PS(OH)-49/PVPy complexes.

solutions of PS(OH)-1, PS(OH)-3, and PS(OH)-5 formed clear mixture solutions when mixed with the chloroform solution of PVPy. The chloroform solutions of PS(OH)-8, PS(OH)-12, PS(OH)-21, PS(OH)-34, and PS(OH)-49 formed gel-like precipitates with the chloroform solution of PVPy. The characteristics of the PS(OH)/PVPy blends with different OH contents are shown in Table 2. The PS(OH)1/PVPy and PS(OH)-3/PVPy blends were immiscible because two distinct glass transition temperatures (T_g's) were observed. The PS(OH)-5/PVPy blend was a miscible blend, showing only one T_g. When the OH content reached or exceeded 8 mol %, PS(OH) and PVPy formed a complex which showed only one T_g. Figure 1 shows the measured T_g and the calculated T_g using the Fox equation[40]

$$\frac{1}{T_{gb}} = \frac{w_1}{T_{g1}} + \frac{w_2}{T_{g2}} \quad (1)$$

where T_{gb} and T_{gi} are the glass transition temperatures of the blend and component i, and w is the weight fraction of the component. When only one T_g was detected, the measured T_g's showed a positive deviation from the calculated values. The higher the OH contents, the larger was the difference between the measured and calculated T_g's, indicating that in PS(OH)/PVPy complexes the mobility of individual chains is greatly reduced[24−27] as a result of the strong hydrogen-bonding interaction between the PS(OH) and PVPy.

XPS Results. The XPS results for all of the PS(OH)/PVPy blend films show the presence of only four elements: carbon, oxygen, fluorine, and nitrogen. No signals from the silicon substrate or other elements were detected, indicating that no contaminants were present and the film thickness was uniformly more than approximately 100 Å. The typical C 1s spectra of the PS(OH)-3/PVPy, PS(OH)-21/PVPy, and PS(OH)-49/PVPy blends can be resolved into five component peaks representing different chemical environments, as shown previously.[41] The five components include a hydrocarbon peak at 285.0 eV, the *C*−N peak at 286.0 eV, the $C-(CF_3)_2OH$ peak at 288.6 eV, the $\pi-\pi^*$ shake-up satellite peak at 291.6 eV, and the CF_3 peak at 293.4 eV.[28,37]

The surface chemical composition of the blends was calculated using the N/C peak area ratio, and the results are shown in Table 2. PS(OH) was found to be enriched at the surface of the immiscible PS/PVPy, PS(OH)-1/PVPy, and PS(OH)-3/PVPy blends because PS(OH) has a much lower surface free energy than PVPy. The surface free energy of PS and PVPy is 40.2 and 68.2 mJ m^{-2}, respectively.[42] For the miscible PS(OH)-5/PVPy blend, the surface was also enriched with PS(OH). However, for the PS(OH)-8/PVPy and PS(OH)-12/PVPy complexes, it was found that PS(OH) was still enriched at the surface, but the surface excess of PS(OH) was much lower compared with the PS(OH)/PVPy blends, with the OH content less than 5 mol %. For the PS(OH)-21/PVPy, PS(OH)-34/PVPy, and PS(OH)-49/PVPy complexes, the chemical compositions of surface and bulk were nearly the same. This indicates that when an interpolymer complex is formed, strong interactions between the functionalities of the polymer chains limit their mobility. Consequently, in this case, the lower surface energy component cannot segregate to the surface.

Figure 2 shows the N 1s core-level spectra of pure PVPy and the blends of PVPy with PS(OH)-5, PS(OH)-

Table 3. N 1s and O 1s Curve-Fitting Results of PS(OH)/PVPy Blends or Compelxes[a]

blends or complexes samples	surface concentration of PS(OH) (mol %)	BE O 1s	fraction of low BE O 1s peak	BE N 1s	fraction of high BE N 1s peak
PS/PVPy	99.6			399.0	0
PS(OH)-1/PVPy	89.3	532.9/534.1	0.57	399.0/399.9	0.01
PS(OH)-3/PVPy	80.8	532.9/534.2	0.74	399.0/399.9	0.02
PS(OH)-5/PVPy	70.7	532.8/534.1	0.83	399.0/399.9	0.05
PS(OH)-8/PVPy	70.4	532.9/534.2	0.95	399.0/399.9	0.13
PS(OH)-12/PVPy	60.8	532.8/534.2	0.96	399.0/399.9	0.16
PS(OH)-21/PVPy	50.9	532.9/534.3	0.97	399.0/400.0	0.21
PS(OH)-34/PVPy	44.3	532.9/534.3	0.97	399.0/400.0	0.25
PS(OH)-49/PVPy	40.5	532.9/534.3	1.00	399.0/399.9	0.32

[a] BE = binding energy.

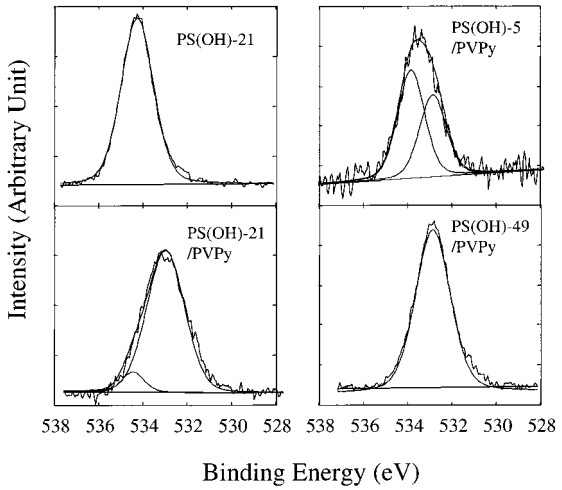

Figure 3. XPS O 1s core-level spectra of pure PS(OH)-21, the PS(OH)-5/PVPy blend, and the PS(OH)-21/PVPy and PS(OH)-49/PVPy complexes.

21, and PS(OH)-49. The N 1s spectrum of PVPy shows a single nitrogen peak with a binding energy of 399.0 eV, which agrees with the previous result.[43] The N 1s spectra of the immiscible blends, PS(OH)-1/PVPy and PS(OH)-3/PVPy, are nearly the same as that of the pure PVPy. In the immiscible blends PS(OH)-1/PVPy and PS(OH)-3/PVPy, PS(OH) and PVPy form separated domains at the surface; consequently, the hydroxyl and pyridyl groups can interact only through hydrogen bonding at the interface between these two phases. Therefore, the N 1s spectrum shows little difference from that of the pure PVPy. However, when the hydroxyl content reaches or exceeds 5 mol %, the N 1s peak of the blends shifts slightly to the higher binding energy side, indicating that the nitrogen in the blends becomes slightly more electropositive because of the formation of more hydrogen bonds. A hydrogen bond is formed by a hydrogen atom that serves a bridge between two electronegative atoms, holding one by a convalent bond and other by purely electrostatic forces. In the current system, the strong positive charge of the hydrogen nucleus of the hydroxyl group is attracted by the negative charge of the nitrogen atom of the pyridyl group. The sharing of the electron cloud between the hydrogen and nitrogen nuclei increases the binding energies of the core levels of the nitrogen atom. Therefore, the N 1s peak of the PS(OH)/PVPy blends with the hydroxyl content higher than 5 mol % can be deconvoluted into two component peaks: one is at 399.0 eV and the other is around 400.0 eV. The high binding energy peak corresponds to the nitrogen atoms involved in the hydrogen bonding. When the hydroxyl content of PS(OH) increases, it is found that N 1s peak shifts to higher binding energy, indicating that the more pyridyl groups in PVPy form hydrogen bonds with the hydroxyl groups of PS(OH). The XPS results further suggest that there is no proton transfer between the hydroxyl and pyridyl groups because the N 1s peak for the positively charged pyridinium ions is at around 401.5 eV.

Table 4. Proposed Structures for Some of the Characteristic Ions in the Positive Spectra of PVPy

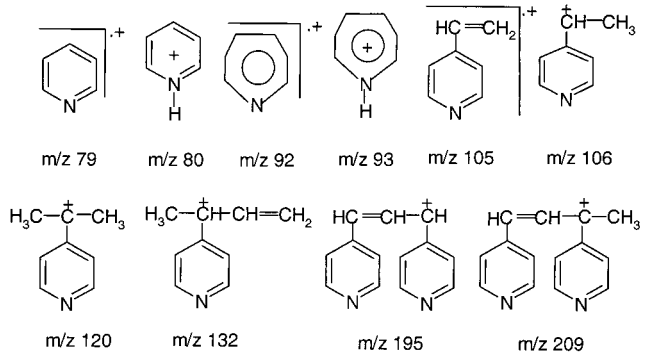

Figure 3 shows the O 1s core-level spectra of PS(OH)-21 and three PS(OH)/PVPy blends with different OH contents. The O 1s electrons of PS(OH) have a binding energy of 534.2 eV. This value is much higher than the binding energy of the O 1s electrons of poly(styrene-*co*-4-vinylphenol) (STVPh) because of the weak hydrogen self-bonding between the hydroxyl groups of PS(OH) due to the presence of bulky trifluoromethyl groups. However, in the PS(OH)/PVPy miscible blends and complexes, the O 1s peak shifts significantly to the low-binding-energy side, indicating that the electron density of the oxygen increases because of the sharing of the electron cloud between the hydrogen and nitrogen nuclei. Each O 1s peak of the PS(OH)/PVPy blends can be deconvoluted into two component peaks: one remains at 534.2 eV, and the other one is around 532.8 eV. The intensity of the O 1s low-binding-energy component peak increases with the hydroxyl content, indicating that more of the hydroxyl groups have interacted with the pyridyl groups via hydrogen bonding in the miscible blend and complexes.

Table 3 shows the curve-fitting results of N 1s and O 1s spectra of PS(OH)/PVPy miscible blends and complexes. The intensity of the low-binding-energy O 1s component peak and the intensity of the high-binding-energy N 1s component peak increases with the hydroxyl content. The fractional share of the low-binding-

Table 5. Ratio of the Absolute Intensity of Some Nitrogen-Containing Peaks to Their Calculated Intensity

secondary ions	PS(OH)-3/PVPy	PS(OH)-5/PVPy	PS(OH)-8/PVPy	PS(OH)-21/PVPy	PS(OH)-49/PVPy
$m/z = 80$	1.06 ± 0.04	1.06 ± 0.04	1.79 ± 0.05	1.69 ± 0.08	1.84 ± 0.05
$m/z = 93$	1.06 ± 0.04	1.05 ± 0.05	1.61 ± 0.05	1.78 ± 0.05	1.75 ± 0.07
$m/z = 106$	0.85 ± 0.05	0.90 ± 0.05	1.56 ± 0.05	1.68 ± 0.07	2.16 ± 0.08
$m/z = 120$	0.73 ± 0.05	0.80 ± 0.04	1.33 ± 0.04	1.72 ± 0.08	1.93 ± 0.06
$m/z = 132$	0.99 ± 0.04	1.03 ± 0.08	1.21 ± 0.06	1.23 ± 0.07	1.13 ± 0.08
$m/z = 195$	1.02 ± 0.07	1.11 ± 0.10	1.27 ± 0.07	1.21 ± 0.07	1.15 ± 0.08
$m/z = 209$	0.78 ± 0.10	0.82 ± 0.08	1.21 ± 0.09	1.26 ± 0.10	1.31 ± 0.08

energy component in the O 1s and N 1s peaks ($\phi_{x,L}$, x = O or N) was calculated using the following equation:

$$\phi_{x,L} = \frac{A_{x,L}}{A_{x,H} + A_{x,L}} \qquad (2)$$

where $A_{x,L}$ and $A_{x,H}$ are the areas of the low-binding-energy and high-binding energy component peaks, respectively. When the hydroxyl content is higher than 21 mol %, the low-binding-energy fraction for the oxygen component is very close to 1, indicating that all the hydroxyl groups of PS(OH) are paired up with all the pyridyl groups of PVPy.

ToF-SIMS Results. Typical ToF-SIMS spectra for PS(OH) have been reported previously.[28] The HFMS monomer can be distinguished from the styrene monomer by the presence of the peaks at m/z = 257, 271, 285, and 373. These ions are directly associated with the HFMS monomer structure. PVPy is distinguished from PS(OH) by the presence of a large peak at m/z = 106[28,37,44]—the largest peak in the PVPy spectrum—and by the presence of characteristic peaks at m/z = 79, 80, 92, 93, 106, 120, 132, 195, and 209. Some possible structures for the nitrogen-containing ions of PVPy are shown in Table 4.

Li and Chan[37] have reported that in poly(styrene-*co*-4-vinylphenol)/poly(strene-*co*-4-vinylpyridine) (STVPh/STVPy) blends the intensity of the peaks at m/z = 80 ($C_5H_6N^+$), 93 ($C_6H_7N^+$), and 106 ($C_6H_6N^+$) is enhanced by the formation of interpolymer complexes. These ions are related to the fragments containing atoms that are involved in the formation of hydrogen bonds. If the hydrogen bonding does not affect the intensity of nitrogen-containing peaks and matrix effects are absent, then the absolute intensities of a given peak in the blends can be calculated by the equation

$$I_{m1,cal} = xI_{m1,PS(OH)} + I_{m1,PVPy}(1 - x) \qquad (3)$$

where $I_{m1,cal}$ is the calculated absolute intensity of the ions at m/z = m1. $I_{m1,PS(OH)}$ and $I_{m1,PVPy}$ are the measured intensities of the ions for the pure PS(OH) and PVPy samples, respectively, and x is the surface molar fraction of PS(OH) determined by the XPS data. The ratio $I_{m1,exp}/I_{m1,cal}$ can be used an indicator of hydrogen bonding. Table 5 is a summary showing the values of $I_{m1,exp}/I_{m1,cal}$ for a series of nitrogen-containing ions. If strong hydrogen bonds are formed between PS(OH) and PVPy, the intensities of the peaks at m/z = 80, 93, and 106 should be greatly enhanced; thus, $I_{m1,exp}/I_{m1,cal}$ should be greater than 1. It is found that in the immiscible PS(OH)-3/PVPy blends the values of $I_{m1,exp}/I_{m1,cal}$ for all the nitrogen-containing ions are close to 1 because PS(OH) and PVPy form separate domains, and the formation of hydrogen bonds is minimal. Even for the miscible blend PS(OH)-5/PVPy, the values of $I_{m1,exp}/I_{m1,cal}$ are still close to 1 because the density of the hydroxyl groups is very low, and only a small number of hydrogen bonds are formed. For the blends such as PS(OH)-8/PVPy, PS(OH)-21/PVPy, and PS(OH)-49/PVPy which form complexes, the values of $I_{m1,exp}/I_{m1,cal}$ for the peaks at m/z = 80, 93, 106, and 120 are much larger than 1. The value of $I_{m1,exp}/I_{m1,cal}$ increases with the hydroxyl content. But for the nitrogen-containing peaks at m/z = 132, 195, and 209, their values of $I_{m1,exp}/I_{m1,cal}$ do not change much with the hydroxyl content. A reexamination of their structures shows that they all contain double bonds; in other words, the formation of these structures is accompanied by a dehydrogenation process which produces an effect countering the effect of hydrogen bonding on the intensities of these peaks, as shown in Scheme 2.

Scheme 2

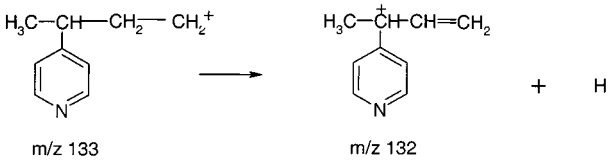

Morphology Evolution during the Transition. Figure 4a presents the total ion, F^-, and CN^- images obtained from the surface of the immiscible PS(OH)-1/PVPy blend. The F^- and CN^- images represent PS(OH)-1 and PVPy, respectively. The F^- and CN^- images are relatively complementary. The total ion images are very uniform. In the immiscible PS(OH)-1/PVPy blend, there are two phases with PVPy forming the dispersed phase with the size ranging from 4 to 6 μm. Figure 4b shows the total ion, F^-, and CN^- images of the immiscible PS(OH)-3/PVPy blend. The miscibility is greatly enhanced, and the PVPy domain size is smaller than the spatial resolution of ToF-SIMS (about 0.5 μm). AFM should be a more sensitive tool to observe the surface morphology of such small sizes. Figure 5 shows the AFM phase images of the PS(OH)-3/PVPy and PS(OH)-5/PVPy blends. It shows that PVPy forms very small domains with size around 40−60 nm. This size is also close to the critical phase separation sizes (about 30−50 nm) at which DSC is just able to detect two discernible T_g's. For miscible PS(OH)-5/PVPy blends, the AFM phase images are nearly uniform, indicating the domain size is extremely small. This result suggests that the surface morphology can be related to the bulk miscibility.

Conclusions

The miscibility of PS(OH) and PVPy blends that can be controlled by adjusting the hydroxyl content has been shown to be an important factor that influences the surface composition of the blends. Miscible blends were formed when the hydroxyl content was less than 3 mol %. Excess of PS(OH) was found at the surface of the immiscible blends. When the hydroxyl content was

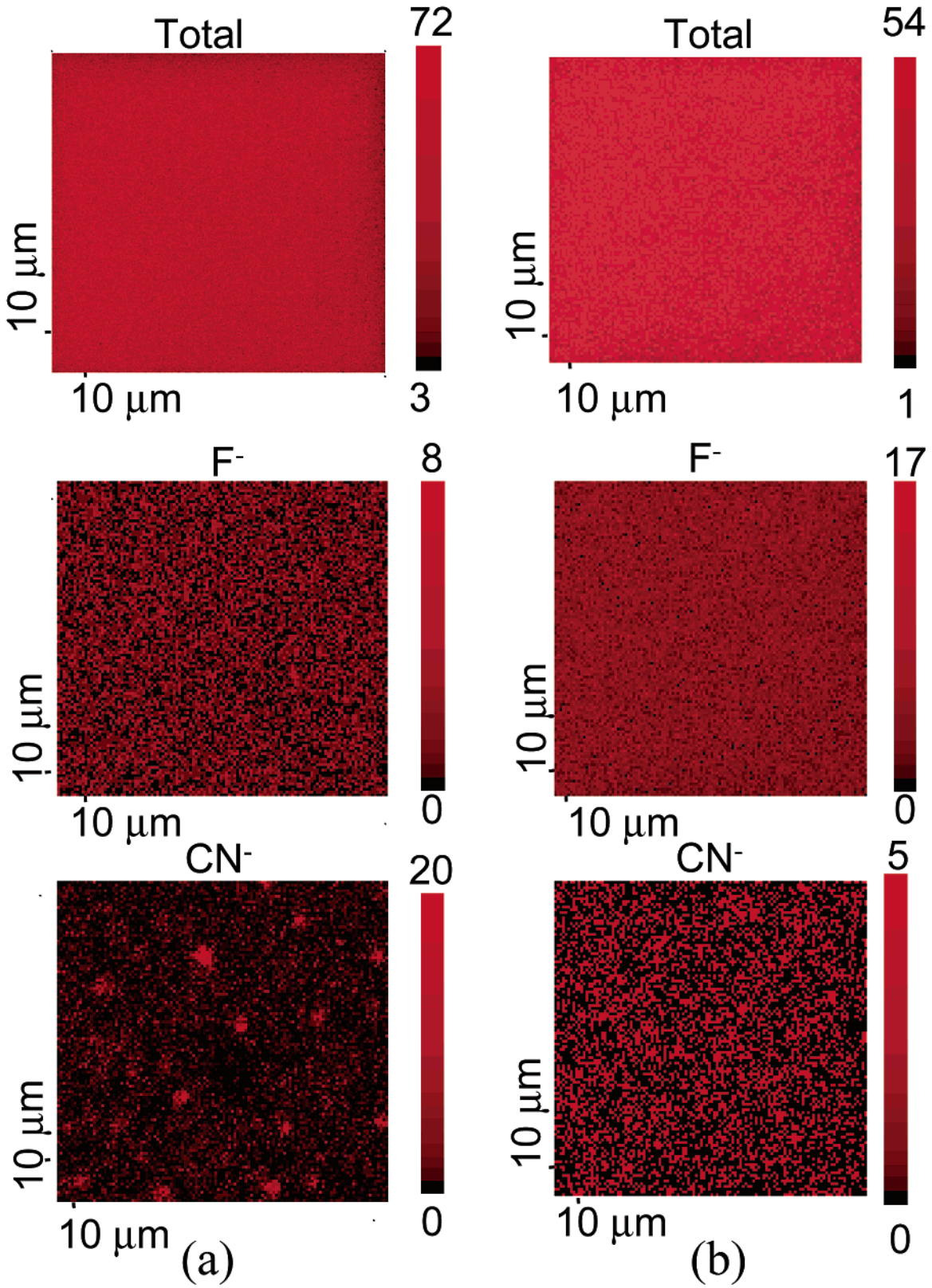

Figure 4. (a) Negative ion images for the PS(OH)-1/PVPy blend. (b) Negative ion images for the PS(OH)-3/PVPy blend.

between 5 and 21 mol %, miscible blends were formed. A gradual increase in the PVPy concentration was observed at the surface and the surface excess of PS-(OH) decreased dramatically. When the hydroxyl content of the PS(OH) was higher than 21 mol %, complexes were formed. The surface and bulk compositions were very similar. XPS results revealed that the intermolecular hydrogen bonding between PS(OH) and PVPy can induce a shift of 0.9−1 and 1.2−1.3 eV in the N 1s and O 1s binding energies, respectively. The hydrogen bonding enhanced the formation of pyridine-ring-containing ions that need to acquire one proton in the

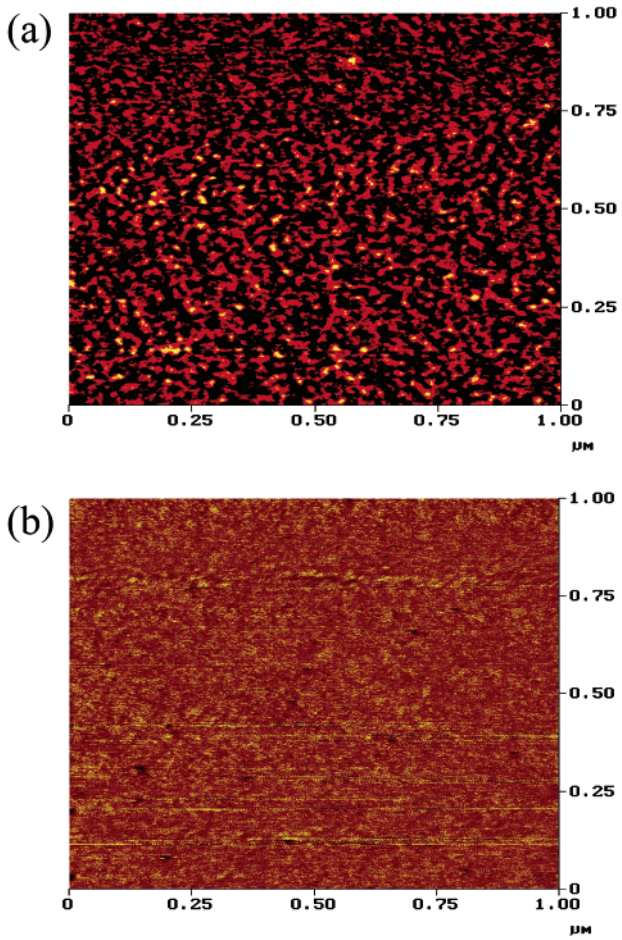

Figure 5. (a) AFM phase image for PS(OH)-3/PVPy blend. (b) AFM phase image for PS(OH)-5/PVPy blend.

process of ion fragmentation. ToF-SIMS imaging and AFM can observe the evolution of phase separation on the surface of PS(OH)/PVPy blends with different hydroxyl contents.

Acknowledgment. This work was supported by National Science Foundation of China and the Hong Kong Government Research Grants Council Joint Research Scheme under Grant No. N_HKUST 618/01 and National Natural Science foundation of China (NNSFC No. 59773023).

References and Notes

(1) Briggs, D.; Kendall, C. R. *Int. J. Adhes. Adhes.* **1982**, *1*, 13.
(2) Pan, D. H.; Prest, W. M. *J. Appl. Phys.* **1985**, *58*, 2861.
(3) Bhatia, Q. S.; Pan, D. H.; Koberstein, J. T. *Macromolecules* **1988**, *21*, 2166.
(4) Jones, R. A. L.; Kramer, E. J.; Rafailovich, M. H.; Sokolov, J.; Schwarz, S. A. *Phys. Rev. Lett.* **1989**, *62*, 280.
(5) Clark, M. B., Jr.; Burkhardt, C. A.; Gardella, J. A., Jr. *Macromolecules* **1989**, *22*, 4495.
(6) Schmidt, J. J.; Gardella, J. A., Jr.; Salvati, L., Jr. *Macromolecules* **1989**, *22*, 4489.
(7) Chilkoti, A.; Ratner, B. D.; Briggs, D. *Chem. Mater.* **1991**, *3*, 51.
(8) Gombotz, W. R.; Hoffman, A. S. *J. Appl. Polym. Sci., Appl. Polym. Symp.* **1988**, *42*, 255.
(9) Thomas, H. R.; O'Malley, J. J. *Macromolecules* **1981**, *14*, 1316.
(10) Schmitt, R. L.; Gardella, J. A.; Salvati, L. *Macromolecules* **1986**, *19*, 648.
(11) Cowie, J. M. G.; Devlin, B. G.; McEwen, I. J. *Polymer* **1993**, *34*, 4130.
(12) Jones, R. A. L.; Kramer, E. J. *Polymer* **1993**, *34*, 115.
(13) Nakanishi, H.; Pincus, P. *J. Chem. Phys.* **1983**, *79*, 997.
(14) Cohen, S. M.; Muthukumar, M. *J. Chem. Phys.* **1989**, *22*, 1689.
(15) Hariharan, A.; Kumar, S. K.; Russell, T. P. *Macromolecules* **1991**, *24*, 4909.
(16) Hariharan, A.; Kumar, S. K.; Russell, T. P. *J. Chem. Phys.* **1993**, *98*, 4163.
(17) Cifra, P.; Bruder, F.; Brenn, R. *J. Chem. Phys.* **1993**, *99*, 4121. Cifra, P. *J. Chem. Phys.* **1992**, *96*, 9157.
(18) Cifra, P. *J. Chem. Phys.* **1992**, *96*, 9157.
(19) Sokolov, J.; Rafailovich, M. H.; Jones, R. A. L.; Kramer, E. *J. Appl. Phys. Lett.* **1989**, *54*, 590.
(20) Hong, P. P.; Boerio, F. J.; Smith, S. D. *Macromolecules* **1994**, *27*, 596.
(21) Tanaka, K.; Yoon, J. S.; Takahara, A.; Kajiyama, T. *Macromolecules* **1995**, *28*, 934.
(22) Painter, P. C.; Park, Y.; Coleman, M. M. *Macromolecules* **1988**, *21*, 66.
(23) Lee, J. Y.; Painter, P. C.; Coleman, M. M. *Macromolecules* **1988**, *21*, 954.
(24) Xiang, M.; Jiang, M.; Zhang, Y.; Wu, C.; Feng, L. *Macromolecules* **1997**, *30*, 2313.
(25) Jiang, M.; Qiu, X.; Qin, W.; Fei, L. *Macromolecules* **1995**, *28*, 730.
(26) Jiang, M.; Li, M.; Xiang, M.; Zhou, H. *Adv. Polym. Sci.* **1999**, *146*, 121.
(27) Liu, Y.; Goh, S. H.; Lee, S. Y.; Huan, C. H. A. *Macromolecules* **1999**, *32*, 1967.
(28) Liu, S.; Weng, L. T.; Chan, C.-M.; Li, L.; Ho, K.-C.; Jiang, M. *Surf. Interface Anal.* **2000**, *29*, 500.
(29) Chan, C. M. *Polymer Surface Modification and Characterization*; Hanser: New York, 1994.
(30) Briggs, D.; Fletcher, I. W.; Reichlmaier, S.; Sanchez, J. L. A.; Short, R. D. *Surf. Interface Anal.* **1996**, *24*, 419.
(31) Briggs, D. *Surface Analysis of Polymers by XPS and Static SIMS*; Cambridge University Press: New York, 1998.
(32) Vanden Eynde, X.; Weng, L. T.; Bertrand, P. *Surf. Interface Anal.* **1997**, *25*, 41.
(33) Galuska, A. A. *Surf. Interface Anal.* **1997**, *25*, 1.
(34) Affrossman, S.; Bertrand, P.; Hartshorne, M.; Kiff, T.; Leonard, D.; Pethrick, R. A.; Richards, R. W. *Macromolecules* **1996**, *29*, 5432.
(35) Lianos, L.; Quet, C.; Due, T. M. *Surf. Interface Anal.* **1994**, *21*, 14.
(36) Li, J. X.; Gardella, J. A., Jr.; McKeown, P. J. *Appl. Surf. Sci.* **1995**, *90*, 205.
(37) Li, L.; Chan, C.-M.; Weng, L. T.; Xiang, M.; Jiang, M. *Macromolecules* **1998**, *31*, 7248.
(38) Cao, X.; Jiang, M.; Yu, T. *Makromol. Chem.* **1989**, *190*, 117.
(39) Liu S.; Zhang, G.; Jiang, M. *Polymer* **1999**, *40*, 5449.
(40) Fox, T. G. *Bull. Am. Phys. Soc.* **1956**, *1*, 123.
(41) Liu, S.; Jiang, M.; Chan, C.-M.; Weng, L.-T. *Macromolecules* **2001**, *34*. 3802.
(42) Jiang, X.; Tanaka, K.; Takahara, A.; Kajiyama, T. *Polymer* **1998**, *39*, 2615.
(43) Zhou, X.; Goh, S. H.; Lee, S. Y.; Tan, K. L. *Appl. Surf. Sci.* **1997**, *119*, 60.
(44) Hook, K. J.; Hook, T. J.; Wandass, J. H.; Gardella, J. A. *Appl. Surf. Sci.* **1990**, *44*, 29.

MA010435M